

Electronic Supplementary Information

Hydrophobic Thin Film Composite Nanofiltration Membranes Derived Solely from Sustainable Resources

Sang-Hee Park¹, Abdulaziz Alammar², Zsolt Fulop¹, Bruno A. Pulido³, Suzana P. Nunes³, Gyorgy Szekely^{1,2,*}

¹Advanced Membranes and Porous Materials Center, Physical Science and Engineering Division (PSE), King Abdullah University of Science and Technology (KAUST), Thuwal, 23955-6900, Saudi Arabia

²Department of Chemical Engineering & Analytical Science, School of Engineering, The University of Manchester, The Mill, Sackville Street, Manchester, M1 3BB, United Kingdom

³Advanced Membranes and Porous Materials Center, Biological and Environmental Science and Engineering Division (BESE), King Abdullah University of Science and Technology (KAUST), Thuwal, 23955-6900, Saudi Arabia

*Corresponding author:
gyorgy.szekely@kaust.edu.sa; gyorgy.szekely@manchester.ac.uk; www.szekelygroup.com

Table of contents

1.	Membrane fabrication	S2
2.	Membrane support characterization	S3
3.	The reaction mechanism of Schiff's base and Michael addition reactions	S4
4.	Membrane characterization	S5
5.	Solvent permeance and MWCO correlation analysis.....	S10
6.	Molecular weight cut off (MWCO).....	S13
7.	Solvent properties.....	S14
8.	Membrane performance	S15
9.	Sustainability analysis	S16
10.	Reference.....	S23

1. Membrane fabrication

Table S1. Reaction conditions of IP reaction of TA and priamine

No.	TA / DI water		Priamine / <i>p</i> -cymene		
	Conc. (mmol/v%)	Immersion time (min)	Conc. (mmol/v%)	Reaction time (min)	
TP-1	1	5	3	0.5	
TP-2				1	
TP-3				2	
TP-4				3	
TP-5				5	
TP-6			0.1	5	
TP-7			0.5		
TP-8			1		
TP-9			5		
TP-10	0.01		0.1		
TP-11	0.05				
TP-12	0.1				
TP-13	0.5				

2. Membrane support characterization

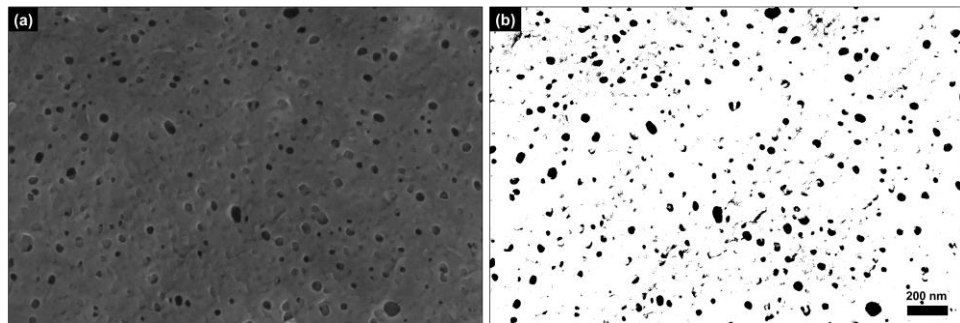


Fig. S1. (a) Surface SEM image and (b) corresponding black/white image of PET support. The surface porosity (black dot, $7\pm2\%$) was calculated from the ImageJ software.

3. The reaction mechanism of Schiff's base and Michael addition reactions

First, the pyrogallol groups of TA could lead to the formation of the highly reactive ortho-quinone and α -hydroxyl-ortho-quinone under weak base conditions. The reactive quinone derivatives could rapidly react with amine groups, which allows to form the covalent bonds of both imine ($-\text{C}=\text{N}-$) and amine ($-\text{C}-\text{NH}-$) by the Schiff's base and Michael addition reaction, respectively (Fig. S2).

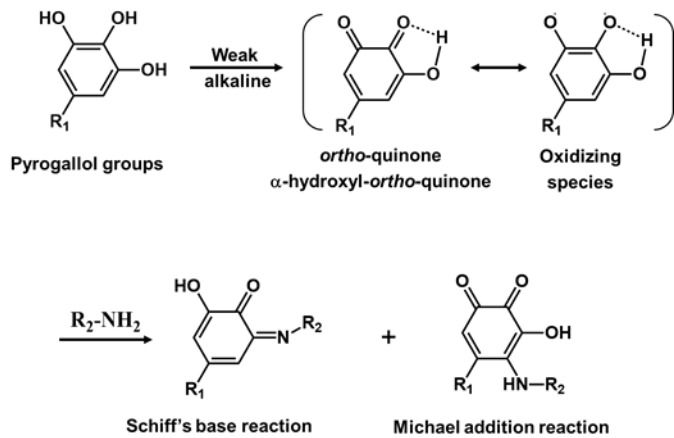


Fig. S2. Reaction mechanism between pyrogallol groups of TA and amine groups of priamine.

4. Membrane characterization

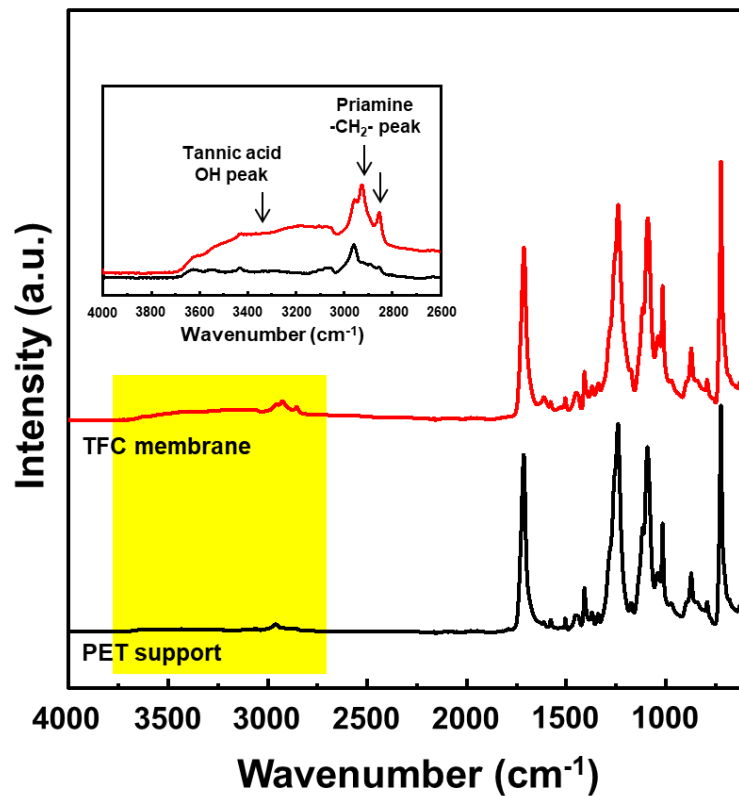


Fig. S3. ATR FT-IR spectra of the PET support and the green TFC membrane prepared from TA concentration (0.1 mmol/v%) and priamine concentration (0.1 mmol/v%).

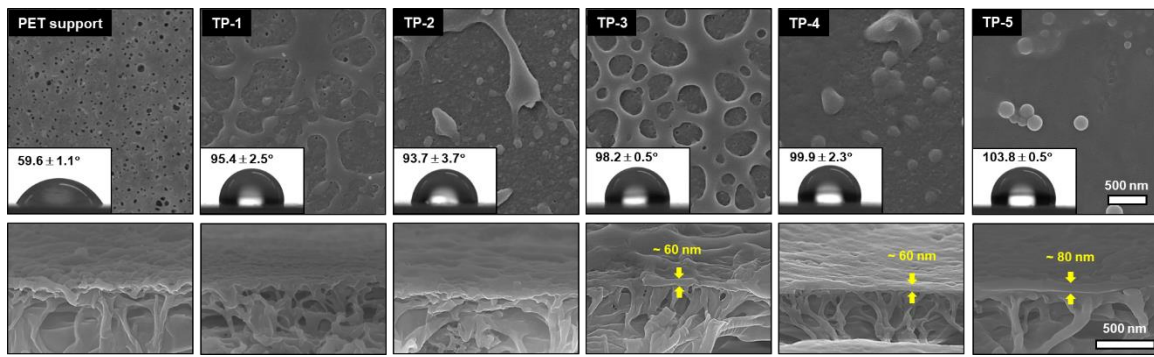


Fig. S4. Surface and cross-sectional SEM images of PET support and the green TFC membranes prepared with different reaction times.

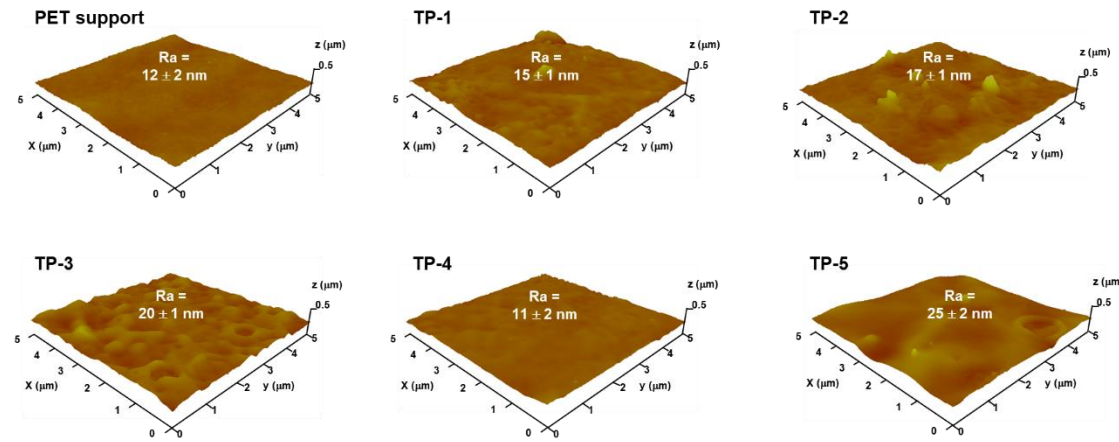


Fig. S5. AFM images of PET support and the green TFC membranes prepared with different reaction times.

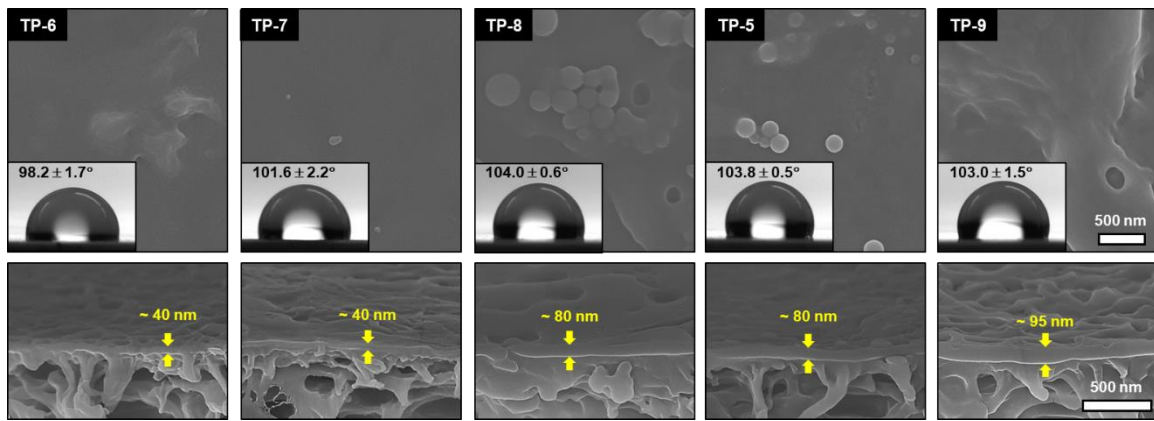


Fig. S6. Surface and cross-sectional SEM images of the green TFC membranes prepared with different Priamine concentrations.

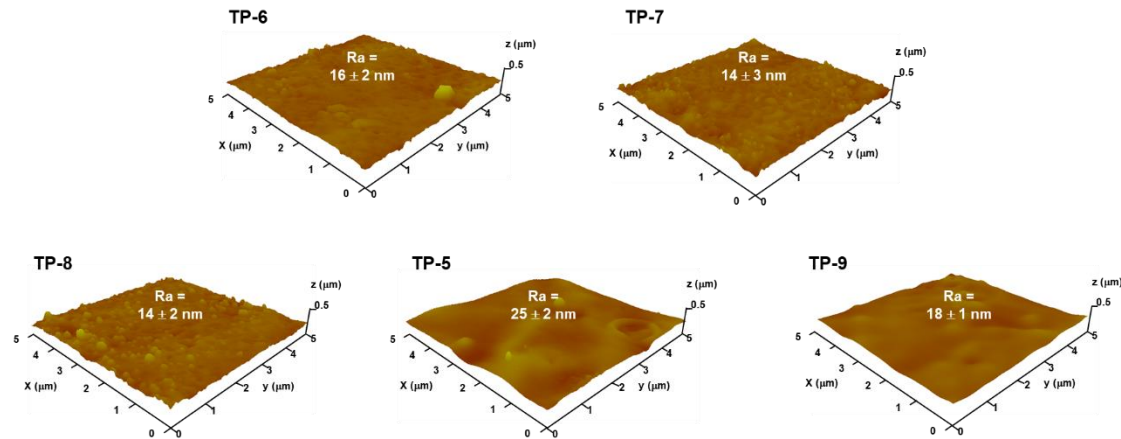


Fig. S7. AFM images of the green TFC membranes prepared with different Priamine concentrations.

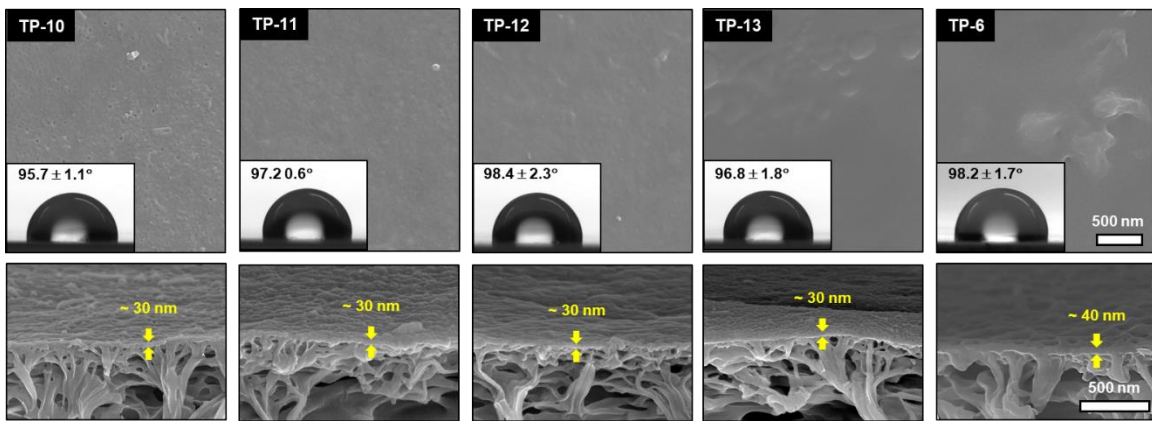


Fig. S8. Surface and cross-sectional SEM images of the green TFC membranes prepared with different TA concentrations.

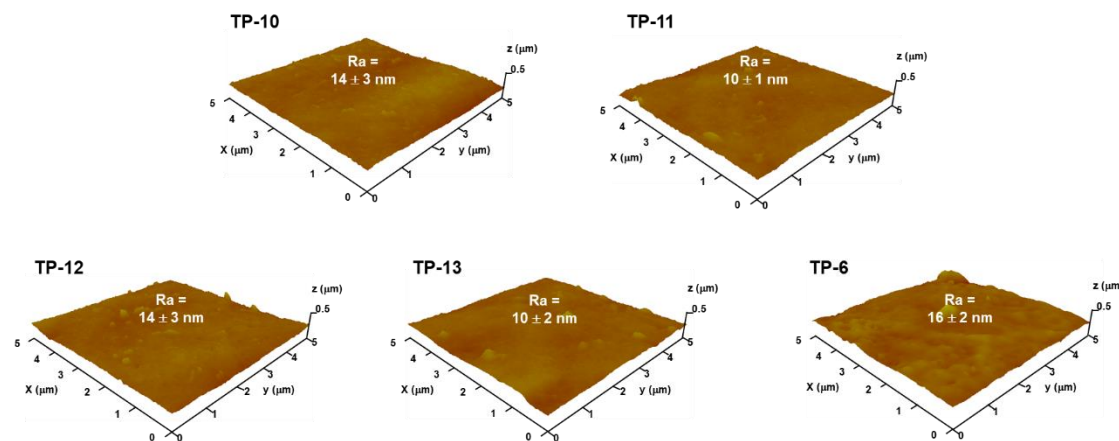


Fig. S9. AFM images of the green TFC membranes prepared with different TA concentrations.

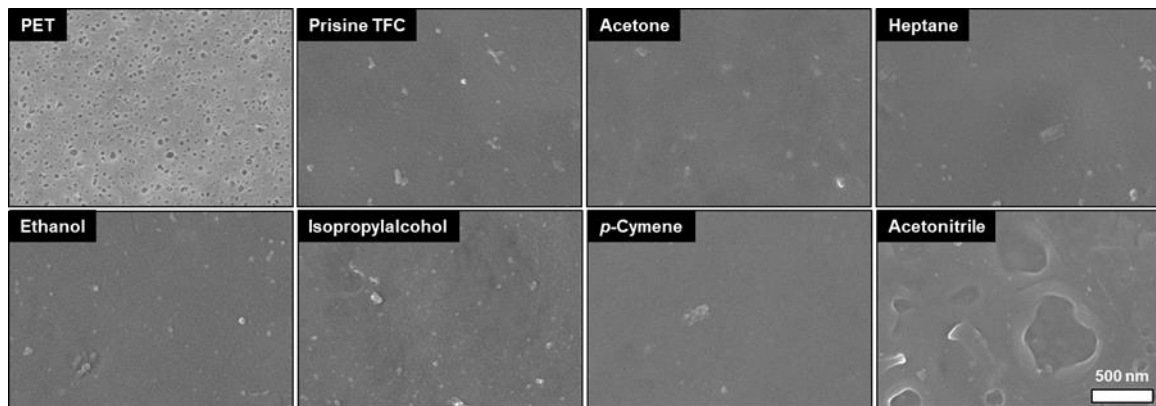


Fig. S10. Surface SEM images of the green TFC membrane prepared from TA concentration (0.1 mmol/v%) and priamine concentration (0.1 mmol/v%) after immersing in each solvent at room temperature for 48 h.

5. Solvent permeance and MWCO correlation analysis

Table S2. Physical properties of acetone

Solvent	MW (Da)	d_m (nm)	η (mPa.s)	V_m (cm 3 mol $^{-1}$)	Density (g mL $^{-1}$)	δ_d (MPa $^{0.5}$)	δ_p (MPa $^{0.5}$)	δ_h (MPa $^{0.5}$)	δ_t (MPa $^{0.5}$)
Acetone	58.08	0.308	0.316	74.166	0.784	15.5	10.4	7.0	19.9

Solvent permeance can be correlated to its physical properties, as suggested by Livingston et al. The solute diameter was obtained using the following equation.

$$d_m = 2 \cdot \left(\frac{3V_m}{4\pi N_A} \right)^{1/3} \quad \text{Eq. S1}$$

where V_m is the molar volume calculated from solvent density, and N_A is the Avogardo's number. To correlate the MWCO data with pore size distribution, the styrene rejection values were used as input data into the pore flow model. The Hagen–Poiseuille equation describes the volumetric flux (J_v) through a membrane comprising uniform capillaries:

$$J_{v,i} = \frac{r_i^2 \Delta P \varepsilon}{8\mu_0 l} \quad \text{Eq. S2}$$

where ε is porosity, ΔP is transmembrane pressure, l is capillary length, μ_0 is solvent bulk viscosity, and r_i is capillary radius. Next, the pore flow rate ($Q_{p,i}$) allows for calculations of the flow through a pore with radius r_i :

$$Q_{p,i} = \frac{\pi r_i^4 \Delta P}{8\mu_0 l} \quad \text{Eq. S3}$$

The overall solute rejection can be calculated using the following set of equations:

$$R_{ij} = 1 - \frac{\Phi_{ij} K_{c,ij}}{1 - (1 - \Phi_{ij} K_{c,ij}) \exp(-P_{c,ij})} \quad \text{Eq. S4}$$

where Φ_{ij} is a partition coefficient, and λ_{ij} is a ratio between the solute radius $r_{s,j}$ (sub-index for a solute is j) and pore radius r_i (sub-index for a pore-size-class in the discrete method is i):

$$\Phi_{ij} = (1 - \lambda_{ij})^2 \quad \text{Eq. S5}$$

$$\lambda_{ij} = \frac{r_{s,j}}{r_i} \quad \text{Eq. S6}$$

therefore, it is assumed that the steric behaviour between the solute and pore wall occurs. Then, the

solute convective $K_{c,ij}$ and diffusive $K_{d,ij}$ hindrance factors are expressed as following:

$$K_{c,ij} = (2 - \Phi_{ij})(1 + 0.054\lambda_{ij} - 0.988\lambda_{ij}^2 + 0.44\lambda_{ij}^3) \quad \text{Eq. S7}$$

$$K_{d,ij} = 1 - 2.3\lambda_{ij} + 1.154\lambda_{ij}^2 + 0.224\lambda_{ij}^3 \quad \text{Eq. S8}$$

The Peclet number ($P_{c,ij}$) characterizing the pore flow is defined as:

$$P_{e,ij} = \frac{K_{c,ij}}{K_{d,ij}D_{s,j}} \left(\frac{r_i^2 \Delta P}{8\mu_{p,i}} \right) \quad \text{Eq. S9}$$

Diffusivity $D_{s,ij}$ of a solute with the radius $r_{s,j}$ is calculated using the Stokes–Einstein equation:

$$D_{s,ij} = \frac{kT}{6\pi\mu_{p,i}r_{s,j}} \quad \text{Eq. S10}$$

where k is the Boltzmann constant and T is temperature. To solve the above equation, the Wilke–Chang formula can be used to estimate the solute diffusivity:

$$D_{s,ij} = 7.4 \times 10^{-8} \frac{T\sqrt{\phi M_{solv}}}{\mu_{p,i} V_{m,j}^{0.6}} \quad \text{Eq. S11}$$

where M_{solv} is the molecular weight (MW) of the solvent molecule, ϕ is a dimensionless solvent parameter and $V_{m,j}$ is the solute molar volume (in $\text{cm}^3 \text{ g mol}^{-1}$).

If rejection $R(r)$ is a continuous function of the pore radius r , PDF $f_{R(r)}$ is introduced to describe the pore size distribution:

$$f_{(r)} = \frac{1}{r\sqrt{2\pi b}} \exp \left[-\frac{(\log \left(\frac{r}{r^*} \right) + \frac{b}{2})^2}{2b} \right] \quad \text{Eq. 12}$$

$$b = \log[1 + (\frac{\sigma}{r^*})^2] \quad \text{Eq. 13}$$

To calculate the function $f_{(r)}$, the mean pore radius (r^*) and the standard deviation (σ) need to be estimated. For simplification, the distribution function is truncated to r_{\max} :

$$\frac{\dot{f}_{R(r)}}{f_{R(r)}} = \frac{1}{\int_0^{r_{\max}} f_{R(r)} dr} \quad \text{Eq. 14}$$

The overall rejection over the pore radii $0 < r < r_{\max}$ can now be calculated using the following expression:

$$R_j = \frac{\int_0^{r_{\max}} \dot{f}_{R(r)} r^4 R(r) \mu(r) dr}{\int_0^{r_{\max}} \dot{f}_{R(r)} r^4 \mu(r) dr} \quad \text{Eq. 15}$$

Implementing the above models, the mean pore size and the standard deviation can be fitted by minimizing the error.

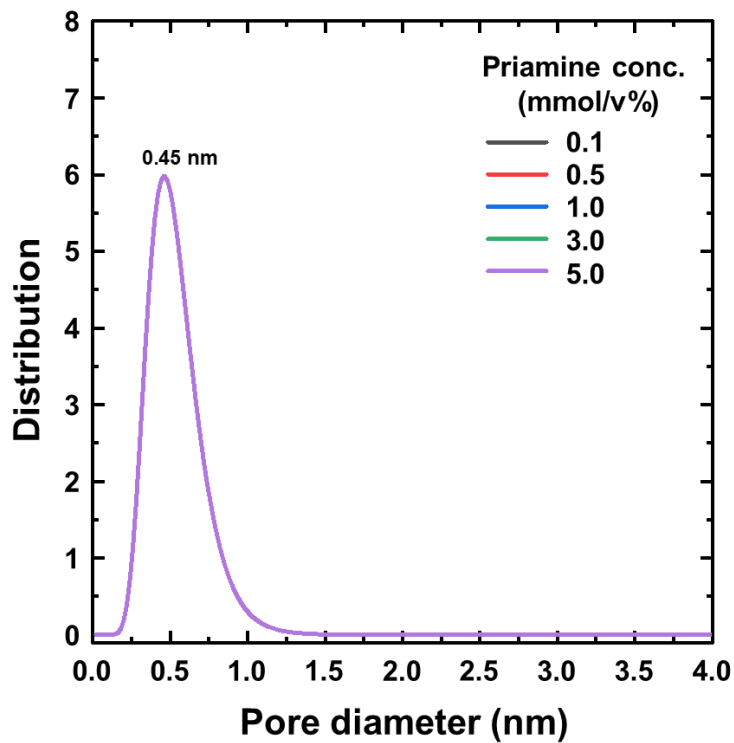


Fig. S11. Pore size of green TFC membranes prepared with different priamine concentration at TA concentration (1.0 mmol/v%) and reaction time (5 min). Note that the pore diameter distribution was found to be identical, hence all the curves overlap.

6. Molecular weight cut off (MWCO)

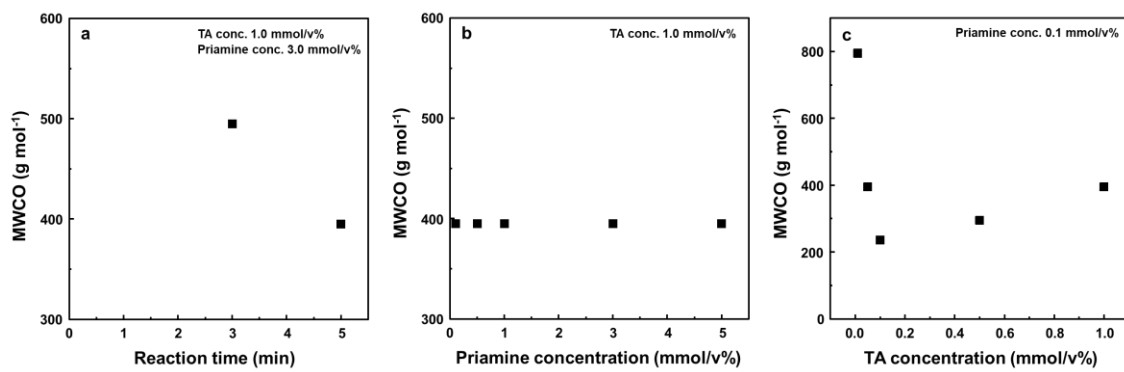


Fig. S12. Molecular weight cut off of green TFC membranes prepared with different (a) reaction times, (b) priamine concentrations and (c) TA concentrations. Note that reaction times less than 3 min did not provide MWCO values because the rejections were lower than 90% (see Fig. 3d).

7. Solvent properties

Table. S3. Hansen solubility parameter and the physical properties of the organic solvent used in this study

Solvent	Molar diameter (d_m , nm)	Viscosity (η , cP) at 25 °C	*Hansen solubility parameter (MPa $^{1/2}$)	
			δ_p (intermolecular force)	$\delta_{p,s} \eta_s^{-1} d_{m,s}^{-2}$
Heptane	0.78	0.37	0	0
Toluene	0.70	0.55	1.4	4.843
Ethanol	0.57	1.22	8.8	21.327
Methyl ethyl ketone	0.66	0.40	9.0	50.393
Acetone	0.62	0.30	10.4	84.547
Acetonitrile	0.55	0.34	18.0	160.822

8. Membrane performance

Table S4. Summary of performance for TFC membranes

No.	Sample Name	Solvent	Permeance (L m ⁻² h ⁻¹ bar ⁻¹)	Styrene dimer (235 g mol ⁻¹) rejection	Pressure (bar)	Temp. (°C)	Reference
1	General TFC		0.3	96			
	General ISA (SM122)		0.6	88			
	Hyphob(1)-TFC-Fa		1.7	97			
	Hyphob(1)-TFC-Si		1.2	97			
	Hyphob(1)-TFC-Fb		0.3	90	30	30	[1]
	Hyphob(2)-TFC-SI		3.83	20			
	Hyphob(2)-TFC		2.85	42			
2	Hyphob(2)-TFC-F		3.63	28			
	S380		3.8	64			
3	Hyphob-TFC-xP84-PEG	Toluene	1.7	97	30	30	[2]
	Hyphob-TFC-PEEK-PEG		2	98			
4	TFC-MPD		0.1	97	30		[3]
	TFN-nanoparticle (300)-M8		0.67	95			
	S122		0.67	88	30	27	[4]
5	Puramem 280		0.67	86			
	S380		3.9	64			
	starmem 240		0.7	33	30	30	[5]
6	(Catechol/POSS)/PI		3.6	-	5	RT	[6]
	O-PASS		2.6	-	6	25	[7]
8	PAN/PEI-Si-X		0.35	-	10	RT	[8]
	Crumpled nanofilm (MPD-3%-1min)		0.3	-	10	30	[9]
10	Crumpled β-CD		1.5	-	10	RT	[10]
	PAN/PEI-TMC		1.9	45			
	PAN/PEI-TMC-PDMS		0.5	50			[11]
12	PIM-1	n-Heptane	4.2	73	10	30	[5]
	PIM-1 film on PAN		4.6	-	13~15	30	[12]
14	O-PASS		2.4	-	6	25	[7]
	Crumpled nanofilm (MPD-3%-1min)		0.5	-	10	30	[9]

9. Sustainability analysis

Table S5. Total mole number of the petroleum-based monomers

No.	Monomer & Additive	Mole number (mmol)	Total mole number (mmol)	Application	Reference
0	Tannic acid Priamine	0.1 0.1	0.2	OSN	This work
1	Resorcinol Trimesoyl chloride	19 0.8	19.8	OSN	[13]
2	<i>m</i> -Penylenediamine Trimesoyl chloride Sodium dodecyl sulfate Triethylamine	19 0.4 0.4 20	39.8	FO	[14]
3	<i>m</i> -Penylenediamine Trimesoyl chloride	14 0.2	14.2	RO	[15]
4	<i>m</i> -Penylenediamine Trimesoyl chloride	37 3.8	40.8	RO	[16]
5	<i>m</i> -Penylenediamine Trimesoyl chloride	19 0.4	19.4	OSN	[3]
6	Piperazine 3,3'5,5'-iphenyl tetraacyl chloride Sodium hydroxide Sodium dodecyl sulfate	6 0.3 3 0.2	9.5	NF	[17]
7	Piperazine Trimesoyl chloride	24 0.8	24.8	NF	[18]
8	Piperazine Trimesoyl chloride <i>N</i> -aminoethyl Piperazine Propane Sulfonate	4 0.8 4.2	9	NF	[19]
9	<i>m</i> -Penylenediamine Trimesoyl chloride Dimethyl sulfoxide Triethylamine Camphorsulfonic acid	19 0.4 26 11 10	66.4	RO	[20]
10	<i>m</i> -Penylenediamine Trimesoyl chloride Triethylamine Sodium dodecyl sulfate	19 0.4 24 1.7	45.1	NF	[21]
11	Polyethyleneimine Trimesoyl chloride	84.4 2.6	87.0	NF	[22]
12	Polyethyleneimine Isophthaloyl dichloride	23.5 0.5	24.0	OSN	[23]
13	Piperazine Trimesoyl chloride	2.3 0.8	3.1	NF	[24]
14	Piperazine Trimesoyl chloride	23.2 0.8	24	NF	[25]
15	<i>m</i> -Penylenediamine Trimesoyl chloride	33.6 0.6	34.2	OSN	[26]

16	<i>m</i> -Penylenediamine Trimesoyl chloride	18.9 0.4	19.3	OSN	[27]
17	<i>m</i> -Penylenediamine Trimesoyl chloride	11.6 0.4	12	OSN	[28]
18	<i>m</i> -Penylenediamine Trimesoyl chloride	18.5 0.4	18.9	OSN	[29]
19	<i>m</i> -Penylenediamine Trimesoyl chloride	18.5 0.4	18.9	OSN	[1]
20	Polyethyleneimine Isophthaloyl dichloride Ehylenediamine	23.5 0.5 33.9	57.9	OSN	[30]
21	Resorcinol Trimesoyl chloride	19 0.8	19.8	OSN	[31]
22	<i>m</i> -Penylenediamine Trimesoyl chloride Sodium dodecyl sulfate Triethylamine	19 0.4 0.4 20	39.8	OSN	[32]
23	<i>m</i> -Penylenediamine Trimesoyl chloride	14 0.2	14.2	OSN	[33]
24	<i>m</i> -Penylenediamine Trimesoyl chloride	37 3.8	40.8	OSN	[34]
25	<i>m</i> -Penylenediamine Trimesoyl chloride	19 0.4	19.4	OSN	[35]

Table S6. Chemical hazard and toxicity of the petroleum-based monomers for TFC membranes

No.	Monomer & Additive	Pictogram	Reference
0	Tannic acid Priamine	This work
1	Resorcinol Trimesoyl chloride		[13]
2	<i>m</i> -Penylenediamine Trimesoyl chloride Sodium dodecyl sulfate Triethylamine		[14]
3	<i>m</i> -Penylenediamine Trimesoyl chloride		[15]
4	<i>m</i> -Penylenediamine Trimesoyl chloride		[16]
5	<i>m</i> -Penylenediamine Trimesoyl chloride		[3]
6	Piperazine 3,3'5,5'-iphenyl tetraacyl chloride Sodium hydroxide Sodium dodecyl sulfate		[17]
7	Piperazine Trimesoyl chloride		[18]
8	Piperazine Trimesoyl chloride <i>N</i> -aminoethyl piperazine Propane sulfonate		[19]
9	<i>m</i> -Penylenediamine Trimesoyl chloride Dimethyl sulfoxide Triethylamine Camphorsulfonic acid		[20]
10	<i>m</i> -Penylenediamine Trimesoyl chloride Triethylamine Sodium dodecyl sulfate		[21]
11	Polyethyleneimine Trimesoyl chloride		[22]
12	Polyethyleneimine Isophthaloyl dichloride		[23]
13	Piperazine Trimesoyl chloride		[24]

No.	Monomer & Additive	Pictogram	Reference
14	Piperazine Trimesoyl chloride		[25]
15	<i>m</i> -Penylenediamine Trimesoyl chloride		[26]
16	<i>m</i> -Penylenediamine Trimesoyl chloride		[27]
17	<i>m</i> -Penylenediamine Trimesoyl chloride		[28]
18	<i>m</i> -Penylenediamine Trimesoyl chloride		[29]
19	<i>m</i> -Penylenediamine Trimesoyl chloride		[1]
20	Polyethyleneimine Isophthaloyl dichloride Ehylenediamine		[30]
21	Resorcinol Trimesoyl chloride		[31]
22	<i>m</i> -Penylenediamine Trimesoyl chloride Sodium dodecyl sulfate Triethylamine		[32]
23	<i>m</i> -Penylenediamine Trimesoyl chloride		[33]
24	<i>m</i> -Penylenediamine Trimesoyl chloride		[34]
25	<i>m</i> -Penylenediamine Trimesoyl chloride		[35]

= 1 mmol

Table S7. Total mole number of the plant-based monomers

No.	Monomer & Additive	Mole number (mmol)	Total mole number (mmol)	Application	Reference
0	Tannic acid Priamine	0.1 0.1	0.2	OSN	This work
1	Tannic acid Cyclohexane-1,4-diamine	0.06 2.19	2.25	NF	[36]
2	Tannic acid Terephthaloyl chloride	0.06 0.49	0.55	OSN	[37]
3	Catechol m-Phenylenediamine	0.91 0.92	1.83	-	[38]
4	Tannic acid Trimesoyl chloride	0.04 0.03	0.07	NF	[39]
5	Quercetin Sodium hydroxide Terephthaloyl chloride	6.62 20 0.99	27.61	OSN	[40]
6	Tannic acid Polyethyleneimine	0.04 4.65	4.69	NF	[41]
7	Morin hydrate Terephthaloyl chloride	6.75 0.99	7.74	OSN	[42]
8	Catechin Sodium hydroxide Terephthaloyl chloride	6.89 20 0.2	27.09	OSN	[43]
9	α -cyclodextrin Sodium hydroxide Trimesoyl chloride	2.06 12.35 0.75	15.16	OSN	[44]

Table S8. Chemical hazard and toxicity of the plant-based monomers for TFC membranes.

No.	Monomer & Additive	Pictogram	Reference
0	Tannic acid Priamine	• • •	This work
1	Tannic acid Cyclohexane-1,4-diamine	! □	[36]
2	Tannic acid Terephthaloyl chloride	□ □ •	[37]
3	Catechol <i>m</i> -Phenylenediamine	! □ □ □	[38]
4	Tannic acid Trimesoyl chloride	• •	[39]
5	Quercetin Sodium hydroxide Terephthaloyl chloride	◆ ◆	[40]
6	Tannic acid Polyethyleneimine	! □	[41]
7	Morin hydrate Terephthaloyl chloride	! □ □	[42]
8	Catechin Sodium hydroxide Terephthaloyl chloride	◆ !	[43]
9	α -cyclodextrin Sodium hydroxide Trimesoyl chloride	◆	[44]

◆ = 1 mmol

Table S9. Comparison of chemical consumption for the fabrication of TFC membrane

No.	Monomer & Additive	Solvent consumption (L m ⁻²)	Monomer consumption (mmol m ⁻²)	Type	Reference
0	Tannic acid Priamine	4	40	Green	This work
1	Tannic acid Cyclohexane-1,4-diamine	4.9	110	Green	[36]
2	Catechin Sodium hydroxide Terephthaloyl chloride	6.1	1658	Green	[43]
3	<i>m</i> -Penylenediamine Trimesoyl chloride	6.7	1226	Petroleum	[45]

10. Reference

1. Jimenez-Solomon, M. F., Gorgojo, P., Munoz-Ibanez, M. & Livingston, A. G. Beneath the surface: Influence of supports on thin film composite membranes by interfacial polymerization for organic solvent nanofiltration. *J. Membr. Sci.* **448**, 102–113 (2013)
2. Jimenez-Solomon, M. F., Bhole, Y. & Livingston, A. G. High flux hydrophobic membranes for organic solvent nanofiltration (OSN) – Interfacial polymerization, surface modification and solvent activation. *J. Membr. Sci.* **434**, 193–203 (2013).
3. Jimenez-Solomon, M. F., Bhole, Y. & Livingston, A. G. High flux membranes for organic solvent nanofiltration (OSN) – Interfacial polymerization with solvent activation. *J. Membr. Sci.* **423–424**, 371–382 (2012).
4. Siddique, H., Peeva, L. G., Stoikos, K., Pasparakis, G., Vamvakaki, M. & Livingston, A. G. Membranes for organic solvent nanofiltration based on preassembled nanoparticles. *Ind. Eng. Chem. Res.* **52**, 1109–1121 (2013).
5. Fritsch, D., Merten, P., Heinrich, K., Lazar, M. & Priske, M. High performance organic solvent nanofiltration membranes: Development and thorough testing of thin film composite membranes made of polymers of intrinsic microporosity (PIMs). *J. Membr. Sci.* **401–402**, 222–231 (2012).
6. Xu, Y. C., Tang, Y. P., Liu, L. F., Guo, Z. H. & Shao, L. Nanocomposite organic solvent nanofiltration membranes by a highly-efficient mussel-inspired co-deposition strategy, *J. Membr. Sci.* **526**, 32–42 (2017).
7. Yuan, S., Wang, J. Li, X., Zhu, J., Volodine, A., Wang, X., Yang, J., Puyvelde, P. V. & Bruggen, B. V., *J. Membr. Sci.*, **549**, 438–445 (2018).
8. Zhang, H., Mao, H., Wang, J., Ding, R. Du, Z., Liu, J. & Cao, S. Mineralization-inspired preparation of composite membranes with polyethyleneimine-nanoparticle hybrid active layer for solvent resistant nanofiltration. *J. Membr. Sci.* **470**, 70–79 (2014).
9. Karan, S., Jiang, Z. & Livingston, A. G. Sub-10 nm polyamide nanofilms with ultrafast solvent transport for molecular separation. *Science* **348**, 1347–1351 (2015).
10. Villalobos, L. F., Huang, T. & Peinemann, K. –V. Cyclodextrin films with fast solvent transport and shape-selective permeability. *Adv. Mater.* **29**, 1606641 (2017).
11. Zhang, H., Zhang, Y., Li, L., Zhao, S., Ni, H., Cao, S. & Wang, J. Cross-linked polyacrylonitrile/polyethyleneimine-polydimethylsiloxane composite membrane for solvent resistance nanofiltration. *Chem. Eng. Sci.* **106**, 157–166 (2014).
12. Gorgojo, P., Karan, S., Wong, H. C., Jimenez-solomon, M. F., Cabral, J. T. & Livingston, A. G. Ultrathin polymer films with intrinsic microporosity: Anomalous solvent permeation and high flux membranes. *Adv. Funct. Mater.* **24**, 4729–4737 (2014).
13. Jimenez-solomon, M. F., Song, Q., Jelfs, K. E., Munoz-Ibanez, M. & Livingston, A. G. Polymer nanofilms with enhanced microporosity by interfacial polymerization. *Nat. Mater.* **15**, 760–767 (2016).
14. Klaysom, C., Hermans, S., Gahlaut, A., Craenenbroeck, S. V. & Vankelecom, I. F. V. Polyamide/ polyacrylonitrile (PA/PAN) thin film composite osmosis membranes: Film optimization, characterization and performance

- evaluation. *J. Membr. Sci.* **445**, 25–33 (2013).
- 15. Xie, W., Geise, G. M., Freeman, B. D., Lee, H. –S., Byun G. & McGrath, J. E. Polyamide interfacial composite membranes prepared from m-phenylenediamine, trimesoyl chloride and a new disulfonated diamine. *J. Membr. Sci.* **403–404**, 152–161 (2012).
 - 16. Park, S. –J., Kwon, S. J., Kwon, H. –E., Shin, M. G., Park, S. –H., Park, H., Park, Y. –I., Nam, S. –E. & Lee, J. –H. Aromatic solvent-assisted interfacial polymerization to prepare high performance thin film composite reverse osmosis membranes based on hydrophilic supports. *Polymer* **144**, 159–167.
 - 17. Wang, H., Zhang, Q. & Zhang, S. Positive charged nanofiltration membrane formed by interfacial polymerization of 3,3',5,5'-biphenyl tetraacyl chloride and piperazine on a poly(acrylonitrile) (PAN) support. *J. Membr. Sci.* **378**, 243–249 (2011).
 - 18. Jahanshahi, M., Rahimpour, A. & Peyravi, M. Developing thin film composite poly(piperazine-amide) and poly(vinyl-alcohol) nanofiltration membranes. *Desalination* **257**, 129–136 (2010).
 - 19. An, Q. –F., Sun W. –D., Zhao, Q., Ji, Y. –L. & Gao, C. –J. Study on novel nanofiltration membrane prepared by interfacial polymerization with zwitterionic amine monomers. *J. Membr. Sci.* **431**, 171–179 (2013).
 - 20. Kim, S. H., Kwak, S. –Y. & Suzuki, T. Positron annihilation spectroscopic evidence to demonstrate the flux-enhancement mechanism in morphology-controlled thin-film-composite (TFC) membrane. *Environ. Sci. Technol.* **39**, 1764–1770 (2005).
 - 21. Shao, L., Cheng, X. Q., Liu, Y., Quan, S., Ma, J., Zhao, S. Z. & Wang, K. Y. Newly developed nanofiltration (NF) composite membranes by interfacial polymerization for safranin O and aniline blue removal. *J. Membr. Sci.* **430**, 96–105 (2013).
 - 22. Wu, D., Huang, Y., Yu, S., Lawless, D & Feng, X. Thin film composite nanofiltration membranes assembled layer-by-layer via interfacial polymerization from polyethylenimine and trimesoyl chloride. *J. Membr. Sci.* **472**, 141–153 (2014).
 - 23. Peyravi, M., Rahimpour, A & Jahanshahi, M. Thin film composite membranes with modified polysulfone supports for organic solvent nanofiltration. *J. Membr. Sci.* **423–424**, 225–237 (2012).
 - 24. Li, Y., Su, Y., Dong, Y., Zhao, X., Jiang, Z., Zhang, R. & Zhao, J. Separation performance of thin-film composite nanofiltration membrane through interfacial polymerization using different amine monomers. *Desalination* **333**, 59–65 (2014).
 - 25. Mis dan, N., Lau, W. J., Ismail, A. F. & Matsuura, T. Formation of thin film composite nanofiltration membrane: Effect of polysulfone substrate characteristics. *Desalination* **329**, 9–18 (2013).
 - 26. Kim, J. H., Moon, S. J., Park, S. H., Cook, M., Livingston, A. G. & Lee, Y. M. A robust thin film composite membrane incorporating thermally rearranged polymer support for organic solvent nanofiltration and pressure retarded osmosis. *J. Membr. Sci.* **550**, 322–331 (2018).
 - 27. Namvar-Mahnoub, M. & Pakizeh, M. Optimization of preparation conditions of polyamide thin film composite membrane for organic solvent nanofiltration. *Korean J. Chem. Eng.* **31**(2), 327–337 (2014).

28. Lu, T., Chen, B., Wang, J., Jia, T., Cao, X., Wang, Y., Xing, W., Lau, C. H. & Sun, S. Electrospun nanofiber substrates that enhance polar solvent separation from organic compounds in thin-film composites. *J. Mater. Chem. A* 6, 15047–15056 (2018).
29. Namvar-Mahboub, M. & Pakizeh, M. Development of a novel thin film composite membrane by interfacial polymerization on polyetherimide/modified SiO₂ support for organic solvent nanofiltration. *Sep. Purif. Tech.* 119, 35–45 (2013).
30. Peyravi, M., Jahanshahi, M., Rahimpour, A., Javadi, A. & Hajavi, S. Novel thin film nanocomposite membranes incorporated with functionalized TiO₂ nanoparticles for organic solvent nanofiltration. *Chem. Eng. J.* 241, 155–166 (2014).
31. Yang, S., Xing, Y., Zhang, J., Su, B., Mandal, B., Gao, X. & Gao, C. Negatively charged polyamide thin film composite membrane with ultra-smooth selective layer and excellent organic solvent resistance for nanofiltration application. *Desalin. Water Treat.* 157, 18–28 (2019).
32. Sun, S. –P. & Chung, T. –S. Enhancement of flux and solvent stability of matrimid® thin-film composite membranes for organic solvent nanofiltration. *AIChE J.* 60, 3623–3633 (2014).
33. Park, S. H., Kim, Y. J., Kwon, S. J., Shin, M. G., Nam, S. E., Cho, Y. H., Park, Y. I., Kim J. F. & Lee, J. –H. Polyethylene battery separator as a porous support for thin film composite organic solvent nanofiltration membranes. *ACS Appl. Mater. Interfaces* 10, 44050–44058 (2018).
34. Duong, P. H. H., Anjum, D. H., Peinemann, K. –V. & Nunes, S. P. Thin porphyrin composite membranes with enhanced organic solvent transport. *J. Membr. Sci.* 563, 684–693 (2018).
35. Xia, L., Ren, J., Weyd, M. & McCutcheon, J. R. Ceramic-supported thin film composite membrane for organic solvent nanofiltration. *J. Membr. Sci.* 563, 857–863 (2018).
36. He, M., Sun, H., Sun, H., Yang, X., Li, P. & Niu, Q. J. Non-organic solvent prepared nanofiltration composite membrane from natural product tannin acid (TA) and cyclohexane-1,4-diamine (CHD). *Sep. Purif. Tech.* 223, 250–259 (2019).
37. Perez-Manriquez, L., Neelakanda, P. & Peinemann, K. –V. Tannin-based thin-film composite membranes for solvent nanofiltration. *J. Membr. Sci.* 541, 137–142 (2017).
38. Qiu, W. –Z., Wu, G. –P. & Xu, Z. –K. Robust coatings via catechol-amine codeposition: Mechanism, kinetics, and application. *ACS Appl. Mater. Interfaces* 10, 5902–5908 (2018).
39. Zhang, Y., Su, Y., Peng, J., Zhao, X., Liu, J., Zhao, J. & Jiang, Z. Composite nanofiltration membranes prepared by interfacial polymerization with natural material tannic acid and trimesoyl chloride. *J. Membr. Sci.* 429, 235–242 (2013).
40. Abdellah, M. H., Perez-Manriquez, L., Puspasari, T., Scholes, C. A., Kentish, S. E. & Peinemann, K. –V. Effective interfacially polymerized polyester solvent resistant nanofiltration membrane from bioderived materials. *Adv. Sustainable Syst.* 2, 1800043 (2018).
41. Li, Q., Liao, Z., Fang, X., Wang, D., Xie, J., Sun, X., Wang, L. & Li, J. Tannic acid-polyethyleneimine crosslinked

- loose nanofiltration membrane for dye/salt mixture separation. *J. Membr. Sci.* 584, 324–332 (2019).
- 42. Perez-Manriquez, L., Neelakanda, P. & Peinemann, K. –V. Morin-based nanofiltration membranes for organic solvent separation processes. *J. Membr. Sci.* 554, 1–5 (2018).
 - 43. Abdellah, M. H., Perez-Manriquez, L., Puspasari, T., Scholes, C. A., Kentish, S. E. & Peinemann, K. –V. A catechin/cellulose composite membrane for organic solvent nanofiltration. *J. Membr. Sci.* 567, 139–145 (2018).
 - 44. Liu, J., Hua, D., Zhang, Y., Japip, S. & Chung T. –S. Precise molecular sieving architectures with janus pathways for both polar and nonpolar molecules. *Adv. Mater.* 30, 1705933 (2018).
 - 45. Paseta, L., Luque-Alled, J. M., Malankowska, M., Navarro, M., Gorgojo, P., Coronas, J. & Tellez, C. Functionalized graphene-based polyamide thin film nanocomposite membranes for organic solvent nanofiltration. *Sep. Purif. Tech.* 247, 116995 (2020).